STRAIN MONITORING FOR HORSETAIL FALLS AND SYLVAN BRIDGES

Final Report

SPR 304-081

by

Steven Soltesz
Oregon Department of Transportation
Research Group

for

Oregon Department of Transportation
Research Group
200 Hawthorne SE, Suite B-240
Salem OR 97301-5192

and

Federal Highway Administration
400 Seventh Street SW, Washington, D.C.20590

May 2002

Technical Report Documentation Page

1. Report No. FHWA-OR-DF-02-17	2. Government Accession No.	3. Recipient's Catalog No.
4. Title and Subtitle STRAIN MONITORING FOR HORSETAIL FALLS AND SYLVAN BRIDGES		5. Report Date May 2002 6. Performing Organization Code
7. Author(s) Steven Soltesz Oregon Department of Transportation Research Group		8. Performing Organization Report No.
9. Performing Organization Name and Address Oregon Department of Transportation Research Group 200 Hawthorne SE, Suite B-240 Salem, Oregon 97301-5192		10. Work Unit No. (TRAIS) 11. Contract or Grant No. SPR 304-081
12. Sponsoring Agency Name and Address Oregon Department of Transportation Research Group 200 Hawthorne SE, Suite B-240 Salem, Oregon 97301-5192 and Federal Highway Administration 400 Seventh Street SW Washington, D.C. 20590		13. Type of Report and Period Covered Final Report 14. Sponsoring Agency Code
15. Supplementary Notes		

16. Abstract

Fiber optic sensors were installed on two reinforced concrete bridges that had been strengthened with fiber reinforced polymer composites. The primary objective for one of the bridges was to provide strain data to verify a computer model for the bridge developed under a separate project. A second objective was to evaluate the effect of fiber reinforced polymer composite reinforcement on bridge response. Unfortunately, usable strain data were not acquired prior to retrofit for either bridge to meet the second objective. This report summarizes the procedures used to install and monitor the sensors and the strain results after the composite retrofit.

17. Key Words FIBER OPTIC, STRAIN, SENSOR, BRIDGE, FIBER REINFORCED, FRP	18. Distribution Statement Copies available from NTIS, and online at http://www.odot.state.or.us/tddresearch		
19. Security Classification (of this report) Unclassified	20. Security Classification (of this page) Unclassified	21. No. of Pages 19 + appendices	22. Price

Technical Report Form DOT F 1700.7 (8-72) Reproduction of completed page authorized Printed on recycled paper

SI* (MODERN METRIC) CONVERSION FACTORS

APPROXIMATE CONVERSIONS TO SI UNITS

Symbol	When You Know	Multiply By	To Find	Symbol
		LENGTH		
In	Inches	25.4	Millimeters	Mm
Ft	Feet	0.305	Meters	M
Yd	Yards	0.914	Meters	M
Mi	Miles	1.61	Kilometers	Km
		AREA		
in^2	Square inches	645.2	millimeters	mm^2
ft^2	Square feet	0.093	meters squared	M^2
yd^2	Square yards	0.836	meters squared	M^2
Ac	Acres	0.405	Hectares	Ha
mi^2	Square miles	2.59	kilometers squared	Km^2
		VOLUME		
fl oz	Fluid ounces	29.57	Milliliters	ML
Gal	Gallons	3.785	Liters	L
ft^3	Cubic feet	0.028	meters cubed	m^3
yd^3	Cubic yards	0.765	meters cubed	m^3
NOTE: Volumes greater than 1000 L shall be shown in m^3.				
		MASS		
Oz	Ounces	28.35	Grams	G
Lb	Pounds	0.454	Kilograms	Kg
T	Short tons (2000 lb)	0.907	Megagrams	Mg
		TEMPERATURE (exact)		
°F	Fahrenheit temperature	5(F-32)/9	Celsius temperature	°C

APPROXIMATE CONVERSIONS FROM SI UNITS

Symbol	When You Know	Multiply By	To Find	Symbol
		LENGTH		
mm	Millimeters	0.039	inches	in
m	Meters	3.28	feet	ft
m	Meters	1.09	yards	yd
km	Kilometers	0.621	miles	mi
		AREA		
mm^2	millimeters squared	0.0016	square inches	in^2
m^2	meters squared	10.764	square feet	ft^2
ha	Hectares	2.47	acres	ac
km^2	kilometers squared	0.386	square miles	mi^2
		VOLUME		
mL	Milliliters	0.034	fluid ounces	fl oz
L	Liters	0.264	gallons	gal
m^3	meters cubed	35.315	cubic feet	ft^3
m^3	meters cubed	1.308	cubic yards	yd^3
		MASS		
g	Grams	0.035	ounces	oz
kg	Kilograms	2.205	pounds	lb
Mg	Megagrams	1.102	short tons (2000 lb)	T
		TEMPERATURE (exact)		
°C	Celsius temperature	1.8C + 32	Fahrenheit	°F

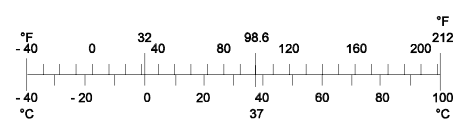

* SI is the symbol for the International System of Measurement

(4-7-94 jbp)

ACKNOWLEDGEMENTS

The author thanks Mr. Marley Kunzler, Mr. Eric Udd, and Mr. Whitten Schulz of Blue Road Research for their input in this project.

DISCLAIMER

This document is disseminated under the sponsorship of the Oregon Department of Transportation and the United States Department of Transportation in the interest of information exchange. The State of Oregon and the United States Government assume no liability of its contents or use thereof.

The contents of this report reflect the view of the authors who are solely responsible for the facts and accuracy of the material presented. The contents do not necessarily reflect the official views of the Oregon Department of Transportation or the United States Department of Transportation.

The State of Oregon and the United States Government do not endorse products of manufacturers. Trademarks or manufacturers' names appear herein only because they are considered essential to the object of this document.

This report does not constitute a standard, specification, or regulation.

STRAIN MONITORING FOR
HORSETAIL FALLS AND SYLVAN BRIDGES

TABLE OF CONTENTS

LIST OF FIGURES

1.0 INTRODUCTION

In 1998, the Oregon Department of Transportation (ODOT) strengthened the historic Horsetail Falls Bridge with fiber reinforced polymer (FRP) composites and initiated research projects to investigate the behavior of the composite-strengthened Bridge (*Kachlakev and McCurry 2000, Kachlakev et al. 2001*). The Bridge is a reinforced concrete (RC) structure on the Historic Columbia Gorge Highway. Since that time, ODOT has been using composites to upgrade other RC bridges to acceptable load capacity levels. However, because the experience with composites on concrete is limited, concerns persist among engineers as to the durability of such retrofits. Field data are needed to determine the long-term operating integrity of concrete structures strengthened with composites.

Vibrating wire strain gauges are durable sensors for long-term monitoring of these structures, but they cannot be used to acquire dynamic strain data. In addition, they have a fairly large footprint that may not be compatible for placement within structural elements. Fiber optic sensors are also durable and can be manufactured without the drawbacks of vibrating wire sensors. Though fiber optic sensing technology is relatively new, it is anticipated that the technology will become an important tool for monitoring the health of roadway structures (*Huston and Fuhr 1995*). Horsetail Falls Bridge was the first experience for ODOT with fiber optic strain sensors. The data were used in a computer model of the Bridge, developed under a separate research project, and for monitoring the bridge response for 3½ years after the composite was installed.

The Sylvan Bridge over Canyon Road on US 26 (ODOT Bridge No. 02285) was strengthened in 2000 with FRP composites and was the second bridge to have fiber optic strain gauges installed. Unlike the Horsetail Falls Bridge, the Sylvan Bridge has several cracks in the beams and is exposed to large traffic volumes. Hence, the use of fiber optic sensors on the Sylvan Bridge was intended to provide data on the effect of composite strengthening on the strain field near a crack as well as on the overall response of the bridge.

1.1 OBJECTIVES

This project had the following objectives:

- Provide strain data to support the computer modeling of the Horsetail Falls Bridge.
- Measure the effect of composite strengthening on bridge response.
- Determine the effect of composite retrofit on the strain in the vicinity of a crack.
- Monitor changes in bridge response over time for a bridge strengthened with FRP composites.

2.0 EXPERIMENTAL METHOD

2.1 SENSOR CONSTRUCTION

The strain sensors used on the Horsetail Falls Bridge and the Sylvan Bridge were based on Bragg gratings (*Kersey, et al. 1997*). Twenty-eight sensors, sixteen with a gauge length of 711 mm and twelve with a gauge length of 1067 mm, were fabricated for the Horsetail Falls Bridge. Ten sensors with a gauge length of 100 mm and four sensors with a gauge length of 1000 mm were fabricated for the Sylvan Bridge. Sensor construction is outlined in Appendix A.

2.2 SENSOR INSTALLATION

Appendix B explains how the sensors were installed on the bridges. For the Horsetail Falls Bridge, 16 sensors were placed at a 45º angle near the end of two beams, and 12 sensors were positioned along the main axis at the bottom of those beams (Appendix C). The intent of the 45º-angle sensors was to monitor the shear strain in the beams; the sensors on the bottom of the beams were to measure flexural strains. Each location had a sensor embedded in the concrete and a sensor attached to the surface of the composite.

For the Sylvan Bridge, all 14 sensors were installed on the same span of the Bridge (Appendix D). Nine of the 100-mm sensors were installed on the Bridge as three rosettes in order to measure principal strain and direction. Two rosettes, one 100-mm sensor, and four 1000-mm sensors were positioned on the center beam because it had more relatively large cracks than the other beams. Rosettes R_2 and R_3 were placed on either side of a crack, and the 100-mm sensor was situated 45º across the crack to monitor the effect of a crack on localized strain fields. The 1000-mm sensors were installed at the beam bottom and just under the bottom of the deck to monitor the neutral axis position. Rosette R_1 was installed on the adjacent beam north of the center beam in the same vicinity from the end of the span and the bottom of the deck as R_2 and R_3 but not in close proximity to any visible cracks.

2.3 STRAIN MEASUREMENT

Initially, the sensing system used on the Horsetail Falls Bridge was capable of measuring static strain with a maximum resolution of 5 microstrain. Using the same sensors, the current instrumentation can provide a 0.02 microstrain resolution with dynamic acquisition rates of approximately 10 KHz (*Schulz, et al. 2002*). An example of strain output from the Horsetail Falls Bridge is shown in Figure 2.1.

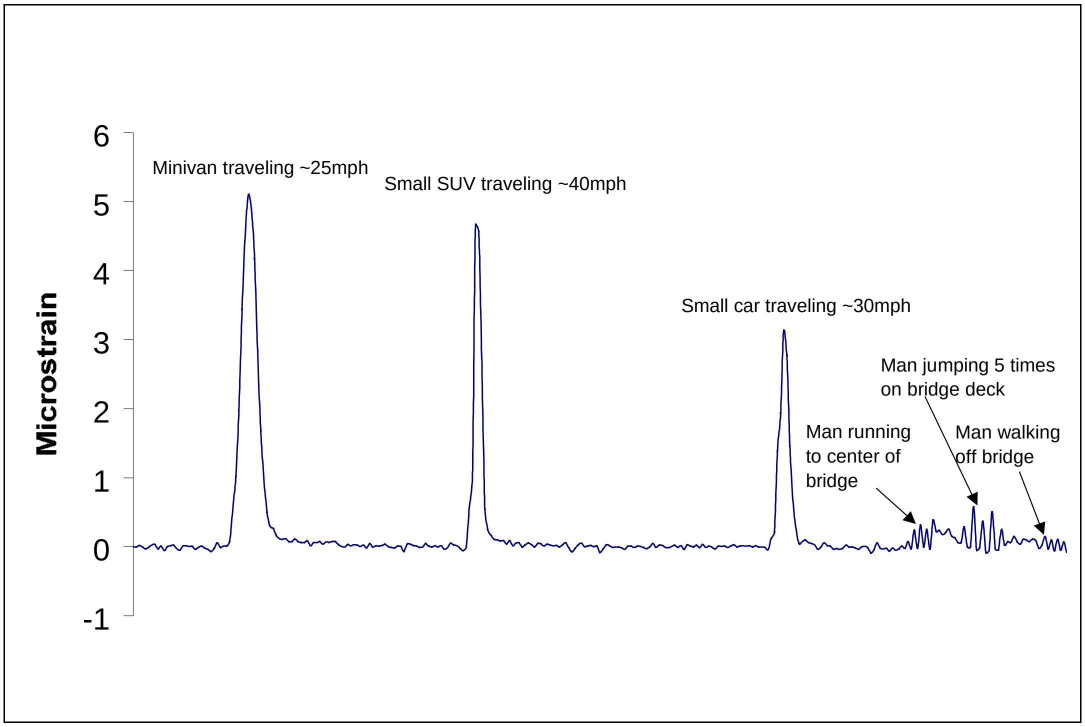

Figure 2.1: An example of strain output from the Horsetail Falls Bridge

Strain measurements were made with instrumentation developed by Blue Road Research. The system interrogates the strain sensors with a broadband light source, and the signals are demodulated with Bragg grating filters (*Schulz, et al. 2002*). Voltage output from the demodulator is captured by a data acquisition system and is later transformed into strain values based on the mathematical characteristics of the Bragg grating filters. Each sensor requires a demodulator with a wavelength-aligned (tuned) filter to convert the waveform to a signal. During the testing, four or eight demodulators were used; consequently, optical fiber leads from the junction box had to be physically switched among the available demodulators in order to monitor all the intended sensors.

The fiber optic instrumentation is able to measure changes in strain using an initial set of measurements as the baseline. An ideal method for determining strain variations is to obtain a baseline with no vehicles on the bridge, and then to use vehicles of known weight to measure the strain response of the bridge. This procedure was used for the Horsetail Falls Bridge in which a baseline measurement for each sensor was made with no traffic on the bridge. Subsequently, a test truck was situated in seven predetermined positions, and strain measurements were collected under these static conditions.

It was not possible to close the Sylvan Bridge because of the high volume of traffic; therefore, the measurements were made under dynamic traffic conditions. The data were collected during periods of relatively low traffic volume and high traffic volume. Four sensors were monitored at one time for two periods of ten minutes. The data sets were noisy and exhibited time-dependent drift; however, the data were manipulated as described in Appendix D to reveal the strain signal.

For both bridges, initial plans called for collecting data before and after installation of the composite. Unfortunately, the state-of-the-art at the time before composite installation on the Horsetail Falls Bridge was such that the fiber optic instrumentation was not sensitive enough to resolve the load-induced strains. For the Sylvan Bridge, there was a window of only a few days in which to acquire the pre-composite data. The instrumentation to accurately acquire dynamic strain data was still evolving at the time; consequently, the time window was not adequate to capture the strain data before installation of the composite. Therefore, no useful data before composite installation was acquired for either bridge.

For the Horsetail Falls Bridge, three sets of data were recorded after the composite was installed. One set of data was obtained from the Sylvan Bridge after the composite was installed.

3.0 RESULTS

3.1 HORSETAIL FALLS BRIDGE

Because the shear-strain sensors crossed through strain gradients, data from these sensors would represent an average strain from the gradient (*Kachlakev and McCurry 2000*). It was decided that this data would have limited value; consequently, no data from the shear sensors were collected. The strain data from the flexural sensors are listed in Appendix C and can be used for comparison in future load testing that may be conducted on the Bridge.

The effect of the composite strengthening on bridge behavior and capacity are reported in two ODOT reports (*Kachlakev and McCurry 2000; Kachlakev, et al. 2001*). Though the composite increased the capacity of the Bridge, finite element analysis showed that the strain due to a loaded dump truck decreased less than six percent with the composite strengthening. Therefore, if strain data had been acquired prior to strengthening, the strains would probably have been similar to those measured after the retrofit.

3.2 SYLVAN BRIDGE

The primary intent of the Sylvan Bridge monitoring was to investigate the change in stress field due to composite strengthening. Though the data before composite strengthening were not obtained, the one set of measurements summarized in Appendix D can be used for comparison to any future testing that may be done on the Bridge.

The largest strain recorded during the monitoring was 22 $\mu\varepsilon$, well below the 1400 $\mu\varepsilon$ typically associated with concrete fracture. As expected, the maximum strain was measured in the flexure zone at the bottom of a beam.

Sets of three sensors had been installed on the Bridge to create rosettes as shown in Appendix D. The intent was to determine principal strains and directions before and after the composite retrofit. The calculated principal strains and directions, however, varied randomly as a function of time. It was surmised that under static or near-static loading conditions, the rosettes would be effective in determining principal strain and direction, but not under the dynamic load conditions of traffic moving at highway speeds.

4.0 SUMMARY

The results obtained from sensors installed on the Horsetail Falls Bridge and the Sylvan Bridge have demonstrated that fiber optic sensors are capable of dynamic strain measurements in civil structures. After being in place for over three years on the Horsetail Falls Bridge, the sensors are still operational, indicative of the anticipated longevity of fiber optic sensors. In the case of Horsetail Falls Bridge, the sensors provided the field data necessary to validate the computer model of the composite-strengthened bridge. As the structure and its composite retrofit age, the sensors will be available to monitor any decline in performance.

The Sylvan Bridge is scheduled for removal in mid-2003. As part of a National Science Foundation project, current plans call for the sensors to measure the effects of damage to the bridge during demolition.

Due to the lack of strain data prior to composite strengthening, the research objectives related to measuring the effect of composite strengthening on bridge response and on strain in the vicinity of a crack were not met.

5.0 REFERENCES

Huston, D.R., and P.L. Fuhr. 1995. “Fiber Optic Smart Civil Structures.” *Fiber Optic Smart Structures*. Eric Udd, Editor. John Wiley Sons, Inc. pp. 647-665.

Kachlakev, D.I., and D.D. McCurry. 2000. Testing of Full-Size Reinforced Concrete Beams Strengthened with FRP Composites: Experimental Results and Design Methods Verification. Oregon Department of Transportation and Federal Highway Administration. Report FHWA-OR-RD-00-19. June.

Kachlakev, D.I., et al. 2001. Finite Element Modeling of Concrete Structures Strengthened with FRP Laminates. Oregon Department of Transportation and Federal Highway Administration. Report FHWA-OR-RD-01-17. May.

Kersey, A.D., et al. 1997. Fiber Grating Sensors. *Journal of Lightwave Technology*. IEEE/OSA. Vol 15, No. 8, August. pp. 1442-1463.

Schulz, W., et al. 2002. Real-Time Damage Assessment of Civil Structures Using Fiber Grating Sensors and Modal Analysis. Proceedings of SPIE Smart Structures Conference 2002, San Diego. To be published summer of 2002.

APPENDICES

APPENDIX A: SENSOR CONSTRUCTION

Appendix A: Sensor Construction

The strain sensors used on the Horsetail Falls Bridge and Sylvan Bridge were based on Bragg gratings. The principal of construction for the sensors was the same for the two bridges; however, the Sylvan sensors were more robust due to improvements in packaging. For the Sylvan sensors, each sensor was housed in a PEEK tube with aluminum end fixtures attached to the optical fiber with epoxy as shown in Figure A.1 below. During fabrication, a constant tension was maintained on the optical fiber so that the fiber is always in tension in the completed sensor. The actual grating is approximately 10 mm long, situated near the center of the sensor. The gauge length is the distance between the points where the fiber is attached to the end-pieces; consequently, the measured strain is the average strain between the end points. Sensors can be constructed with any gauge length, from slightly larger than the length of the Bragg grating to, in principle, many meters. A finished sensor is shown in Figure A.2 below.

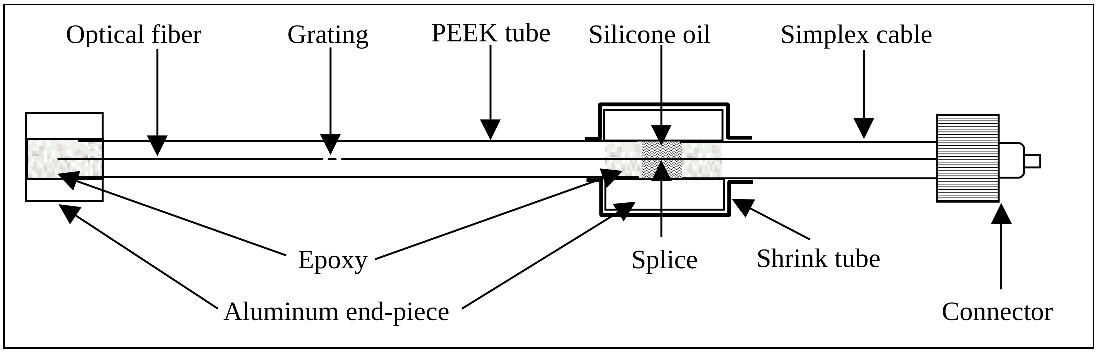

Figure A.1: Schematic of sensor construction (not to scale)

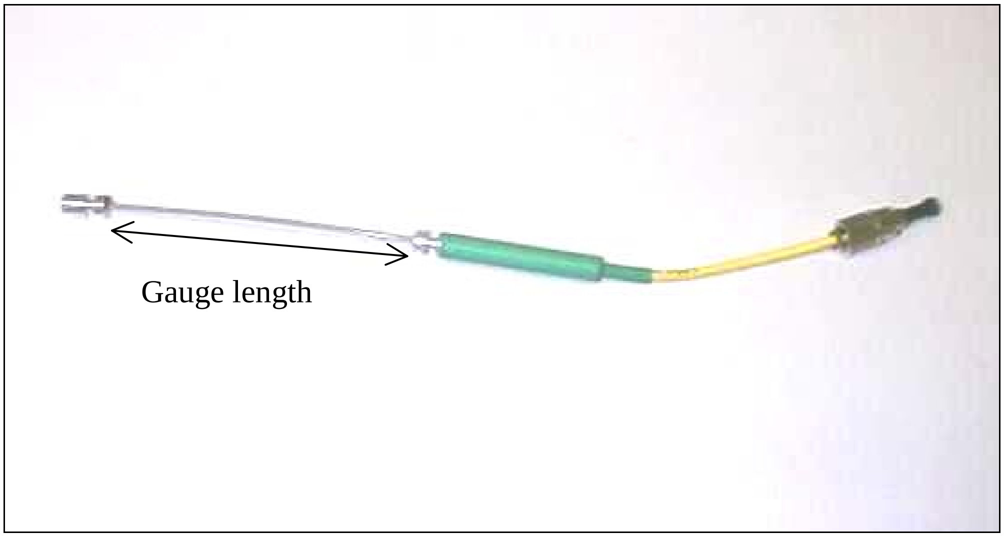

Figure A.2: View of a 100 mm gauge-length sensor installed on the Sylvan Bridge

APPENDIX B: SENSOR INSTALLATION

Appendix B: Sensor Installation

Sensor installation for the Sylvan Bridge consisted of the following steps:

1. Locations of the sensors, optical fiber leads, and the junction box were marked on the Bridge.
2. Grooves approximately 8 mm wide and 15 mm deep were cut for the sensors and optical fiber leads.
3. Sensors and leads were fixed in place with Epcon A7 epoxy and duct tape as shown in Figure B.1 below. All optical fiber leads were fed into the junction box shown in Figure B.2 below.
4. Grooves were filled with Renderoc HBA mortar and smoothed out flush with the surface of the concrete as shown in Figure B.3 below.
5. FRP composite material was placed over the sensors.

For Horsetail Falls Bridge, the sensors were installed in a similar manner, with additional sensors attached to the surface of the FRP composite with epoxy.

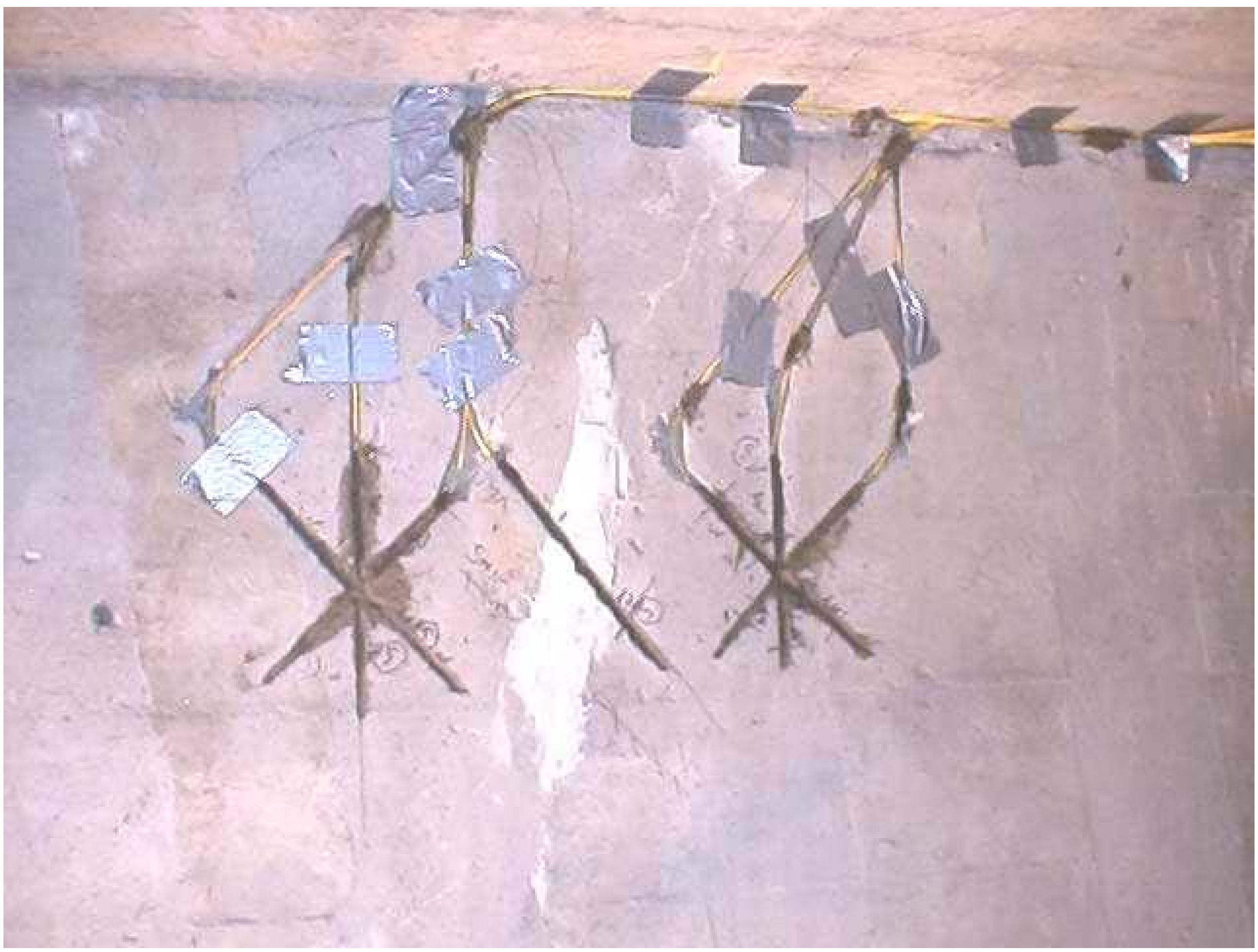

Figure B.1: Sensors fixed in grooves with epoxy

Figure B.2: Junction box

Figure B.3: Appearance of sensor locations after the grooves were filled with grout

APPENDIX C: HORSETAIL FALLS BRIDGE

Appendix C1: Plan view showing the two instrumented beams. (Not to scale)

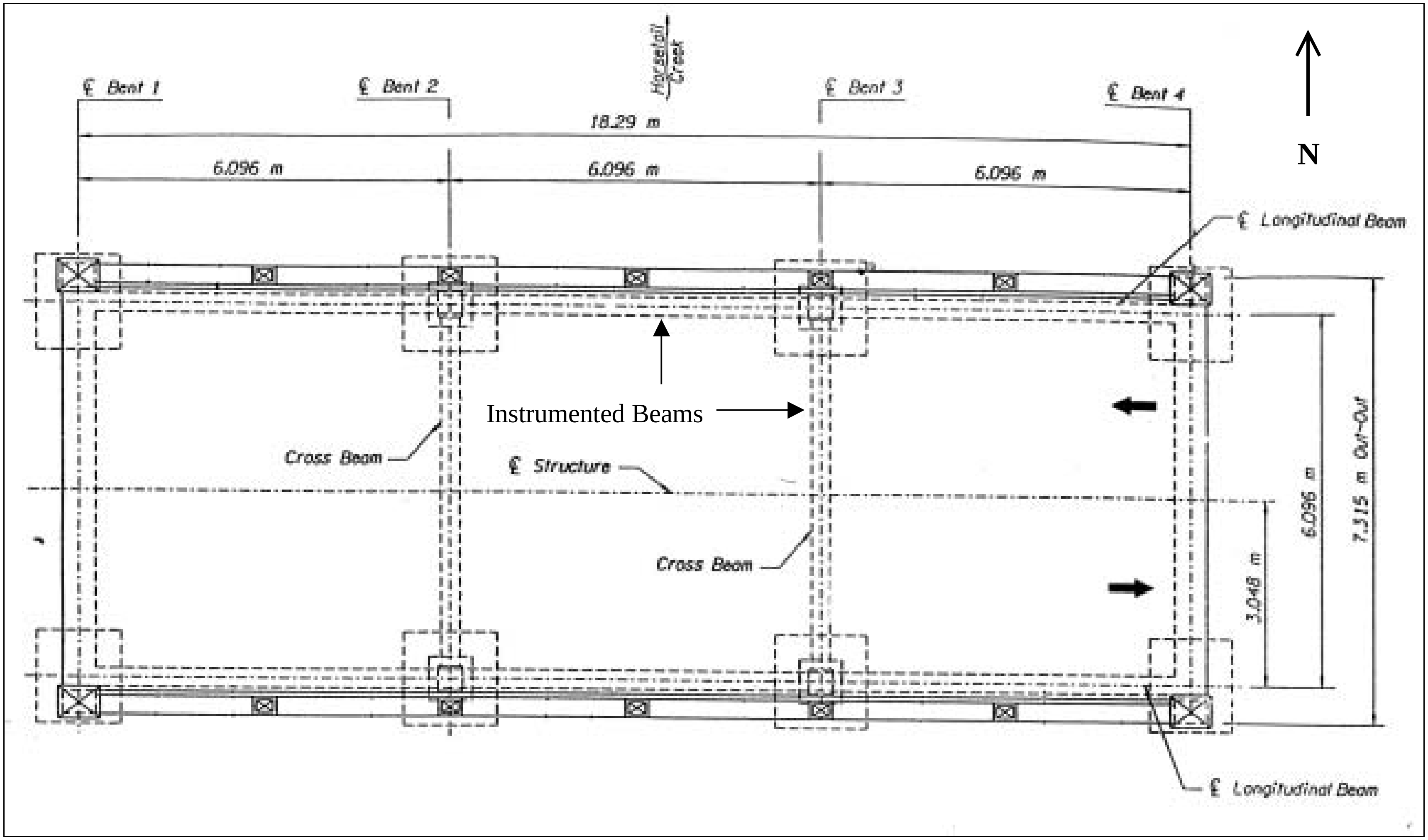

Appendix C2: Fiber optic sensor positions

Each indicated location includes two sensors: one embedded in the concrete and one attached to the surface of the FRP composite. Specific sensor locations are distinguished with a four- or five-digit alphanumeric label (e.g., L0SRA, T1FC). All dimensions are in millimeters.

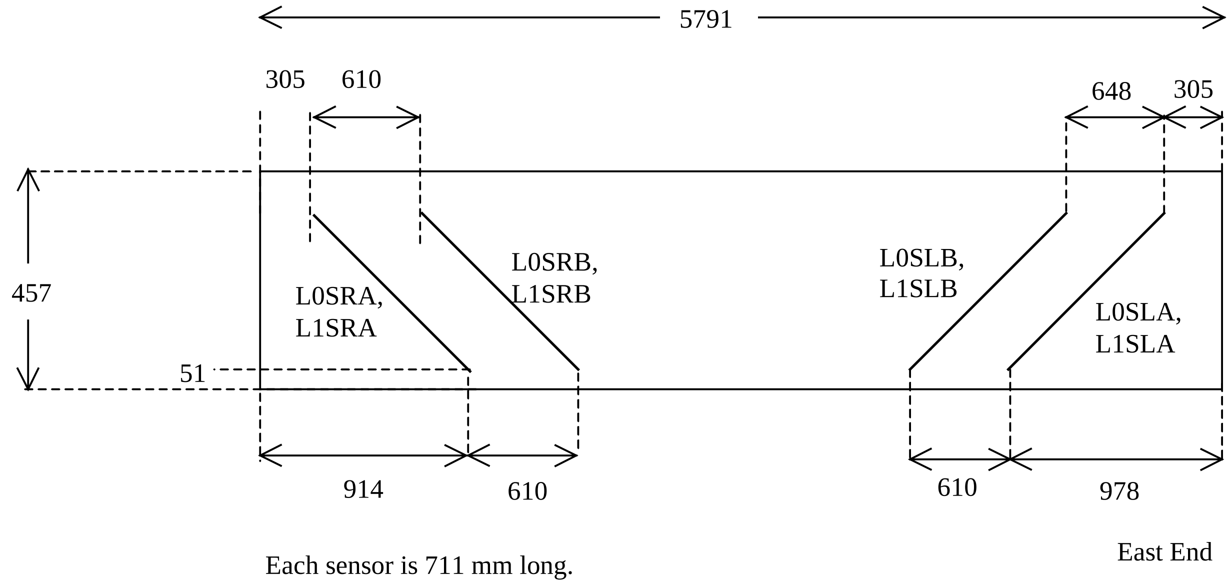

Each sensor is 711 mm long.

Longitudinal beam, side view, observer facing north
Note: In the sensor location designation, 0 refers to embedded in concrete and 1 refers to on the surface of the composite.

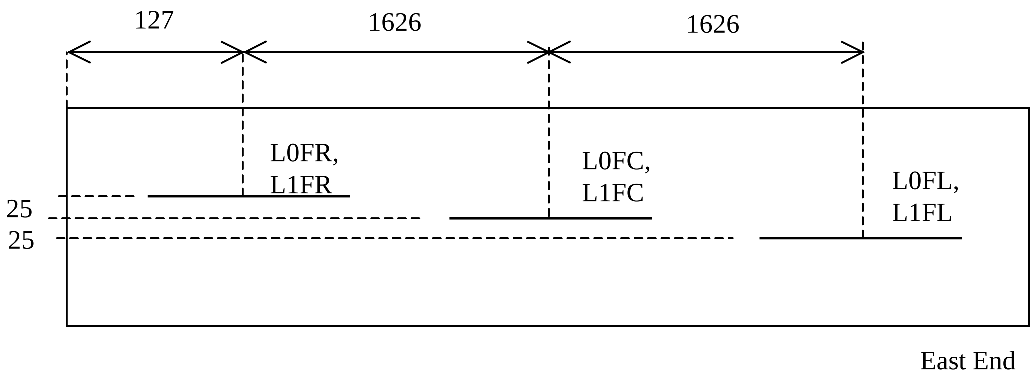

Each sensor is 1067 mm long.

Longitudinal beam, observer looking up at the bottom

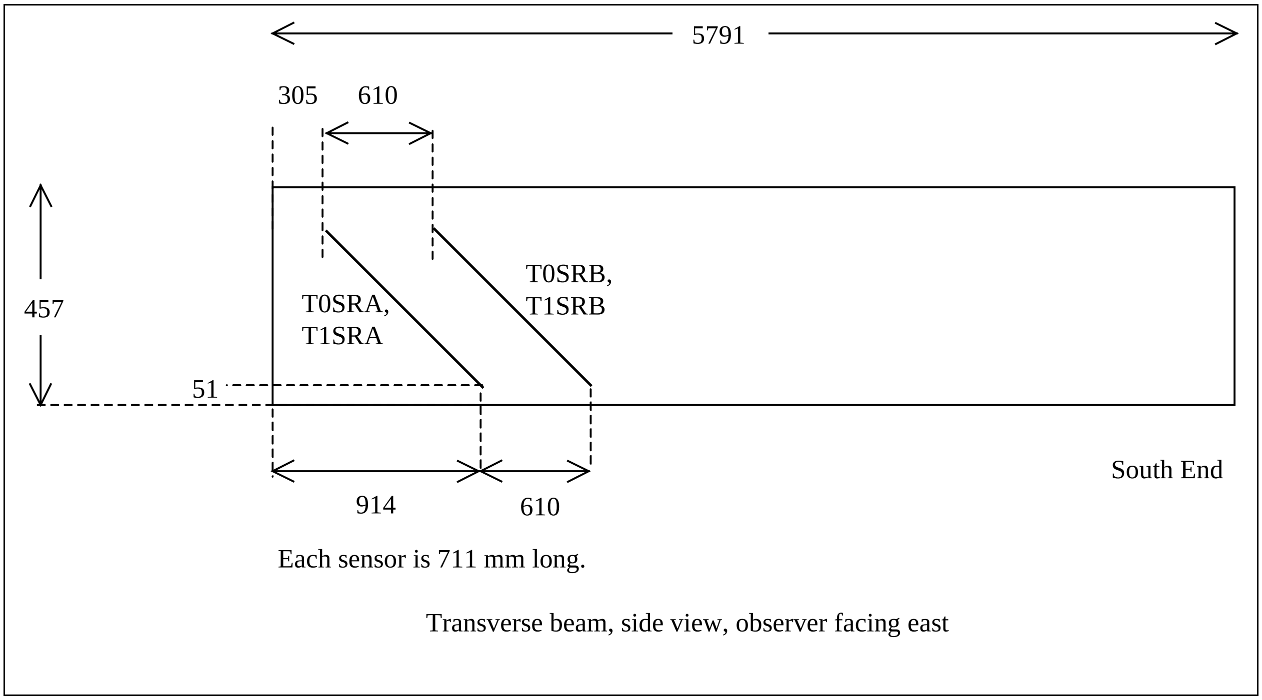
5791
305
610
457
T0SRA,
T1SRA
T0SRB,
T1SRB
51
914
610
South End
Each sensor is 711 mm long.
Transverse beam, side view, observer facing east

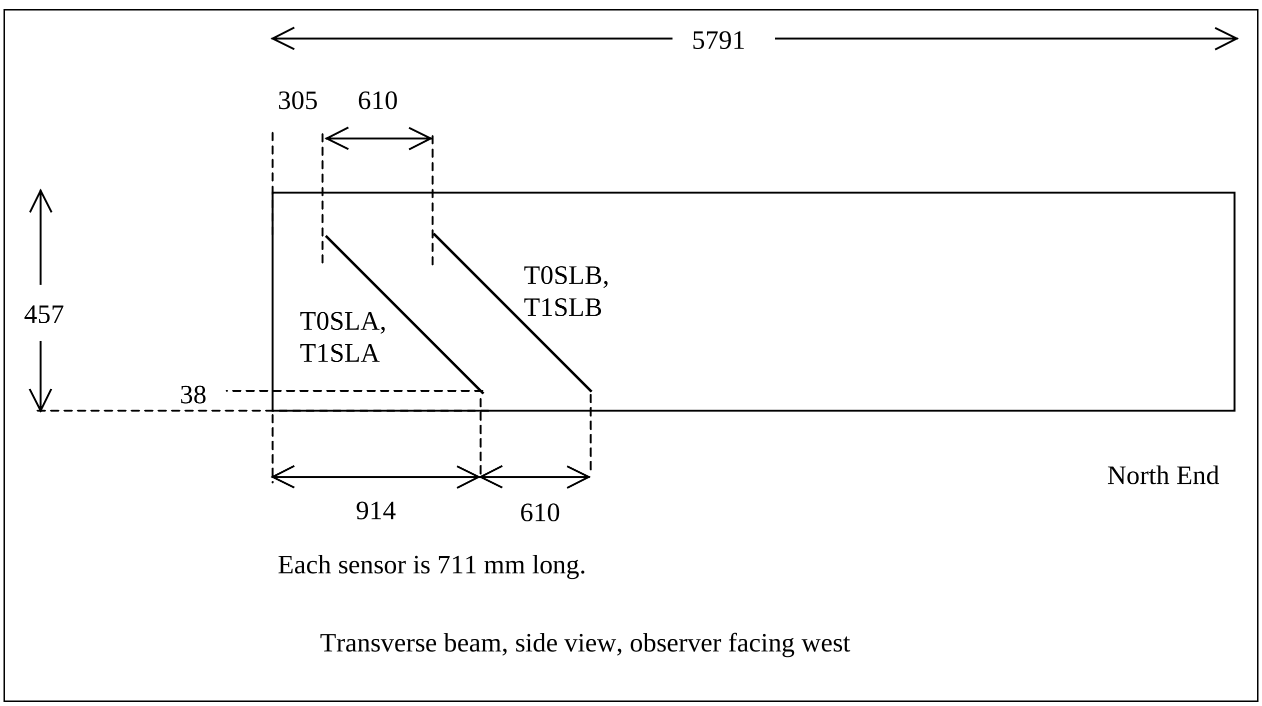
5791
305
610
457
T0SLA,
T1SLA
T0SLB,
T1SLB
38
914
610
North End
Each sensor is 711 mm long.
Transverse beam, side view, observer facing west

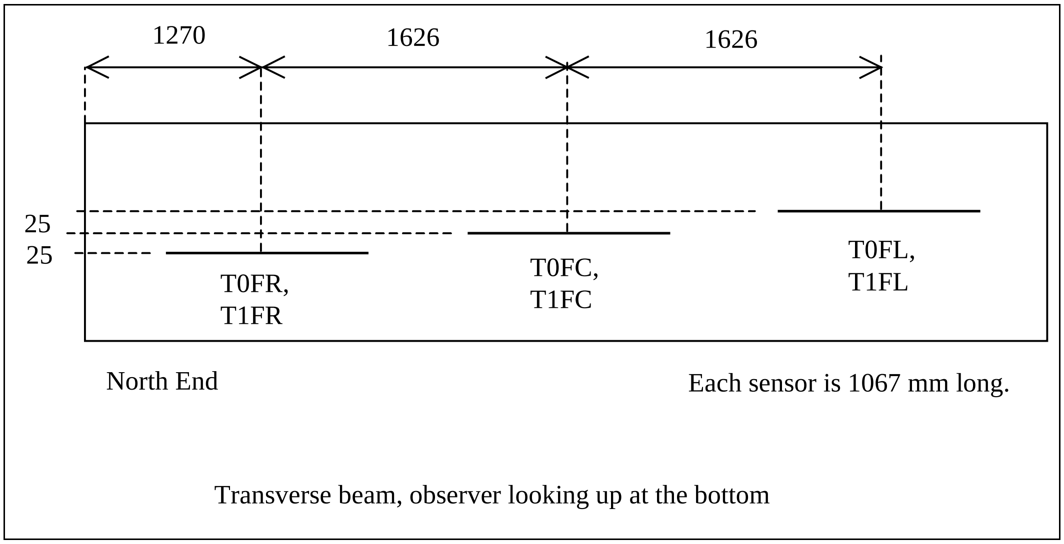
1270
1626
1626
25
25
T0FR,
T1FR
T0FC,
T1FC
T0FL,
T1FL
North End
Each sensor is 1067 mm long.
Transverse beam, observer looking up at the bottom

Appendix C3: Sensor locations and associated sensor numbers

Sensor Location	Sensor Number
T0FL	17
T0FC	13
T0FR	14
T1FL	39
T1FC	40
T1FR	36
T0SRA	26
T0SRB	25
T0SLA	21
T0SLB	19
T1SRA	28
T1SRB	34
T1SLA	29
T1SLB	30
L0FL	15
L0FC	12
L0FR	18
L1FL	37
L1FC	38
L1FR	35
L0SRA	20
L0SRB	23
L0SLA	22
L0SLB	10
L1SRA	B16
L1SRB	27
L1SLA	33
L1SLB	32

Appendix C4: Truck positions during load testing.

(Dimensions in millimeters)

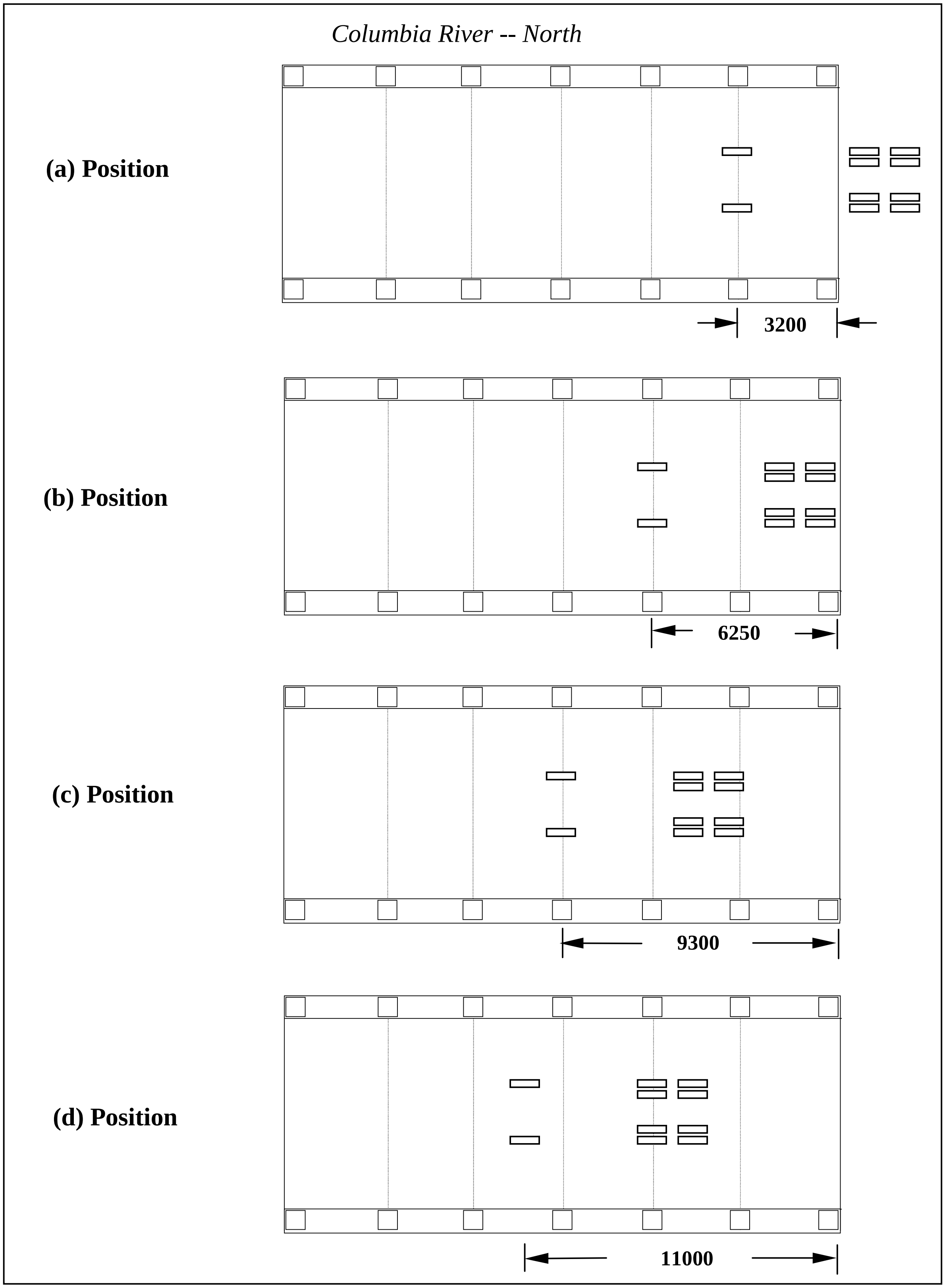

(e) Position 5

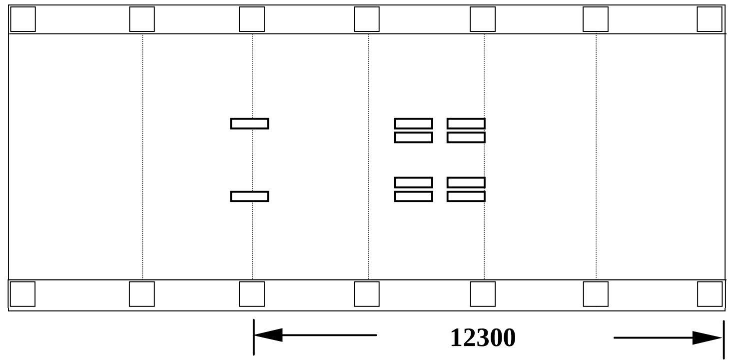

(f) Position 6

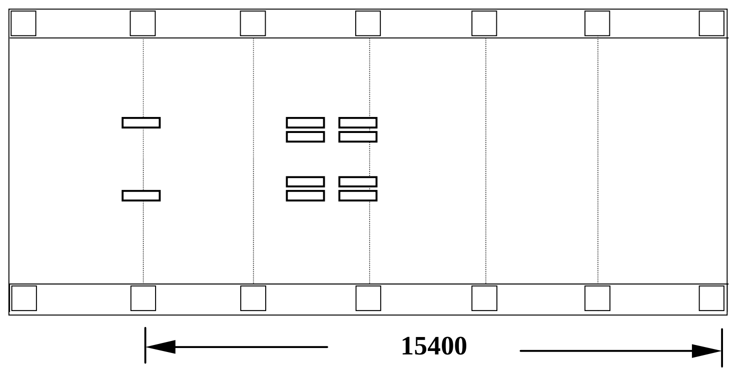

(g) Position 7

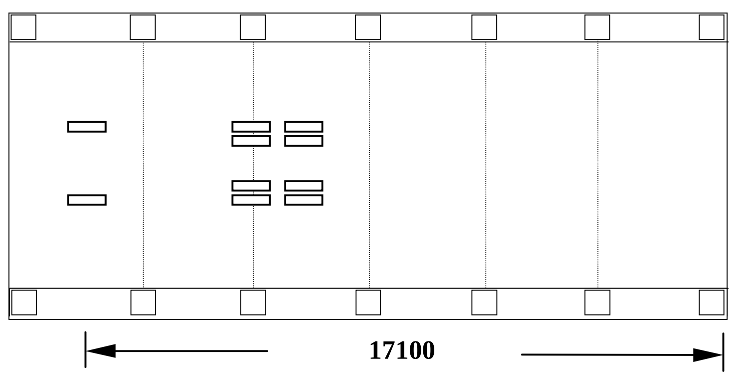

Appendix C5: Truck details

November 1999 Test (All dimensions in millimeters)

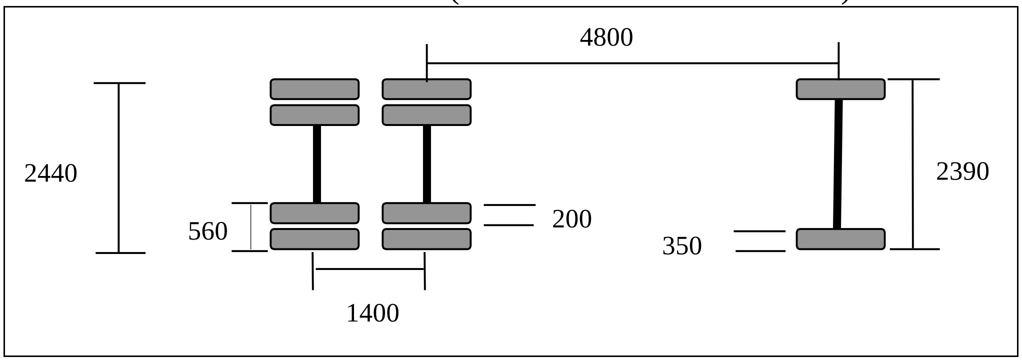

Axle weights in Newtons (pounds)

<u>Empty</u>:
- Front: 56,900 (12,800)
- Center: 32,000 (7200)
- Back: 31,100 (7000)

<u>Full</u>:
- Front: 68,900 (15,500)
- Center: 70,300 (15,800)
- Back: 69,400 (15,600)

November 2000 Test (All dimensions in millimeters)

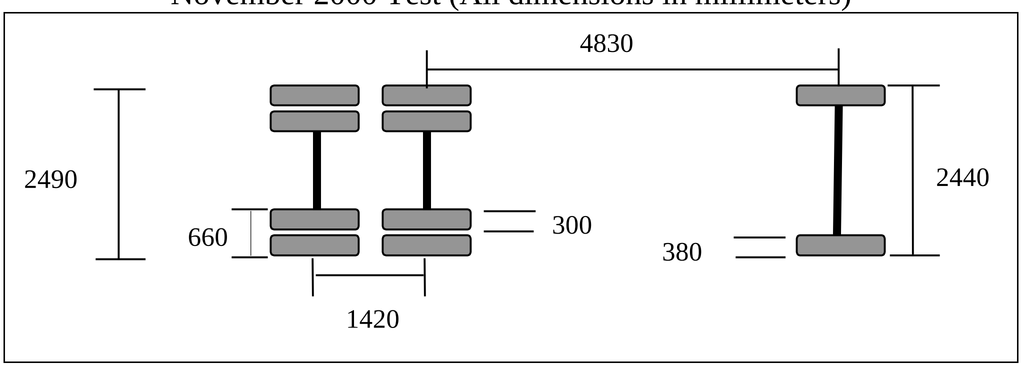

Axle weights in Newtons (pounds)

<u>Empty</u>:
- Front: 56,900 (12800)
- Center: 33,400 (7500)
- Back: 31,100 (7000)

<u>Full</u>:
- Front: 69,400 (15,600)
- Center: 75,200 (16,900)
- Back: 73,800 (16,600)

February 2001 Test (All dimensions in millimeters)

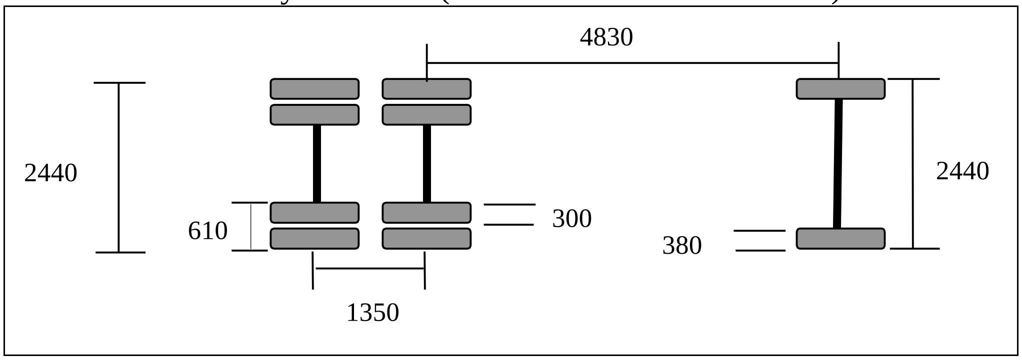

Axle weights in Newtons (pounds)

Empty:

Front: 72,000 (16200)
Center: 32,500 (7300)
Back: 31,600 (7100)

Full:

Front: 78,700 (17,700)
Center: 57,800 (13,000)
Back: 56,000 (12,600)

Appendix C6: Strain results

November 1999 test
Four sensors read simultaneously.

Truck Condition	Position	Strain per Location (με)			
		T0FC	L0FC	T1FC	T1FR
Empty	1	3	-1	4	3
Empty	2	7	0	7	7
Empty	3	7	2	8	8
Empty	4	8	1	9	9
Empty	5	7	1	8	8
Empty	6	3	2	5	4
Empty	7	1	0	2	3
Empty	1	3	-1	4	3
Empty	2	7	0	7	7
Empty	3	8	3	7	7
Empty	4	8	2	8	8
Empty	5	7	2	7	7
Empty	6	3	3	4	3
Empty	7	1	1	1	2

Truck Condition	Position	Strain per Location (με)			
		L0FL	L0FR	L1FC	T0FR
Full	1	-2	0	-1	5
Full	2	-1	0	-1	12
Full	3	-2	0	3	17
Full	4	1	1	3	20
Full	5	4	0	4	19
Full	6	2	1	7	10
Full	7	0	1	4	5
Full	1	-2	0	-1	5
Full	2	-1	0	-1	12
Full	3	-2	0	3	17
Full	4	0	1	3	19
Full	5	4	0	4	19
Full	6	2	1	7	10
Full	7	0	1	3	4

Truck Condition	Position	Strain per Location (με)			
		L0FL	L0FR	L1FC	T0FR
Empty	1	-2	0	-1	4
Empty	2	0	0	0	9
Empty	3	0	1	3	10
Empty	4	0	1	2	10
Empty	5	2	0	2	9
Empty	6	1	1	3	5
Empty	7	0	1	1	2
Empty	1		0	-1	4
Empty	2		0	0	8
Empty	3		0	3	9
Empty	4		1	2	10
Empty	5		0	2	9
Empty	6		0	3	4
Empty	7		0	1	2

Truck Condition	Position	Strain per Location (με)			
		T0FC	L0FC	T1FC	T1FR
Full	1	3	-15	4	1
Full	2	9	-1	8	3
Full	3	16		10	4
Full	4	20	3	11	4
Full	5	19	6	11	4
Full	6	6	9	6	1
Full	7	3	3	3	0
Full	1	3	-2	4	1
Full	2	9	-1	7	3
Full	3	16	3	10	4
Full	4	20	3	11	5
Full	5	19	7	10	5
Full	6	6	10	6	2
Full	7	2	3	3	1

November 2000 test
Eight sensors read simultaneously

Truck Condition	Position	Strain per Location (με)							
		T0FC	L0FC	T1FC	T1FR	L0FL	L0FR	L1FC	T0FR
Empty	1	17	0	19	10	-2	0	0	8
Empty	2	37	4	40	25	-2	1	2	14
Empty	3	40	9	43	31	-4	4	11	17
Empty	4	43	8	45	35	1	7	8	25
Empty	5	40	9	42	30	3	4	8	22
Empty	6	18	10	22	10	-1	4	11	5
Empty	7	8	6	13	9	-1	5	6	0
Full	1	18	-4	18	13	-4	-1	-3	8
Full	2	52	-2	45	35	0	-1	-2	27
Full	3	78	6	71	55	-3	4	8	37
Full	4	92	5	86	61	2	6	6	42
Full	5	86	11	79	57	11	3	16	38
Full	6	32	19	31	22	8	10	22	19
Full	7	12	6	12	8	2	7	7	9

February 2001 Test
Eight sensors read simultaneously

Truck Condition	Position	Strain per Location (με)							
		T0FC	L0FC	T1FC	T1FR	L0FL	L0FR	L1FC	T0FR
Empty	1	16	-6	23	NA	-5	-2	-4	8
Empty	2	42	0	44	NA	1	-2	-1	22
Empty	3	45	9	45	NA	1	4	10	20
Empty	4	45	6	46	NA	3	7	7	22
Empty	5	42	8	42	NA	6	3	6	22
Empty	6	21	8	22	NA	4	4	10	9
Empty	7	9	3	11	NA	3	3	4	5
Full	1	21	-4	20	NA	-5	-2	-2	12
Full	2	49	0	49	NA	-3	-2	0	29
Full	3	63	8	60	NA	-1	2	10	33
Full	4	71	6	69	NA	4	6	8	37
Full	5	66	11	64	NA	8	2	10	39
Full	6	29	15	28	NA	4	7	18	17
Full	7	13	5	12	NA	2	4	6	8

APPENDIX D: SYLVAN BRIDGE

Appendix D1: Plan view showing the position of the strain sensors

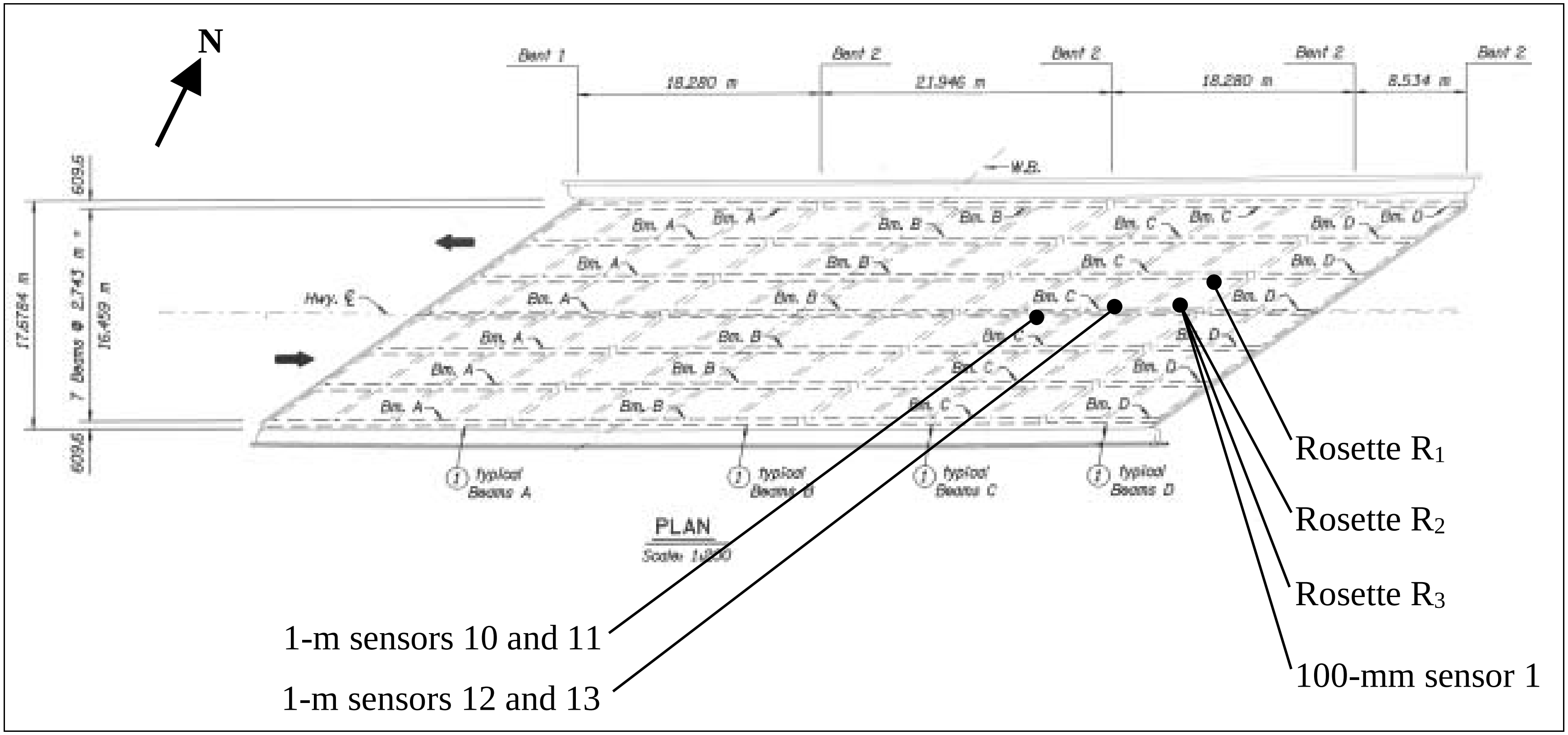

Appendix D2: Fiber optic sensor positions

Position of 100 mm sensors on center beam. All dimensions are in millimeters. The italicized numbers are sensor identification numbers, and the italicized Rs are rosette identification labels.

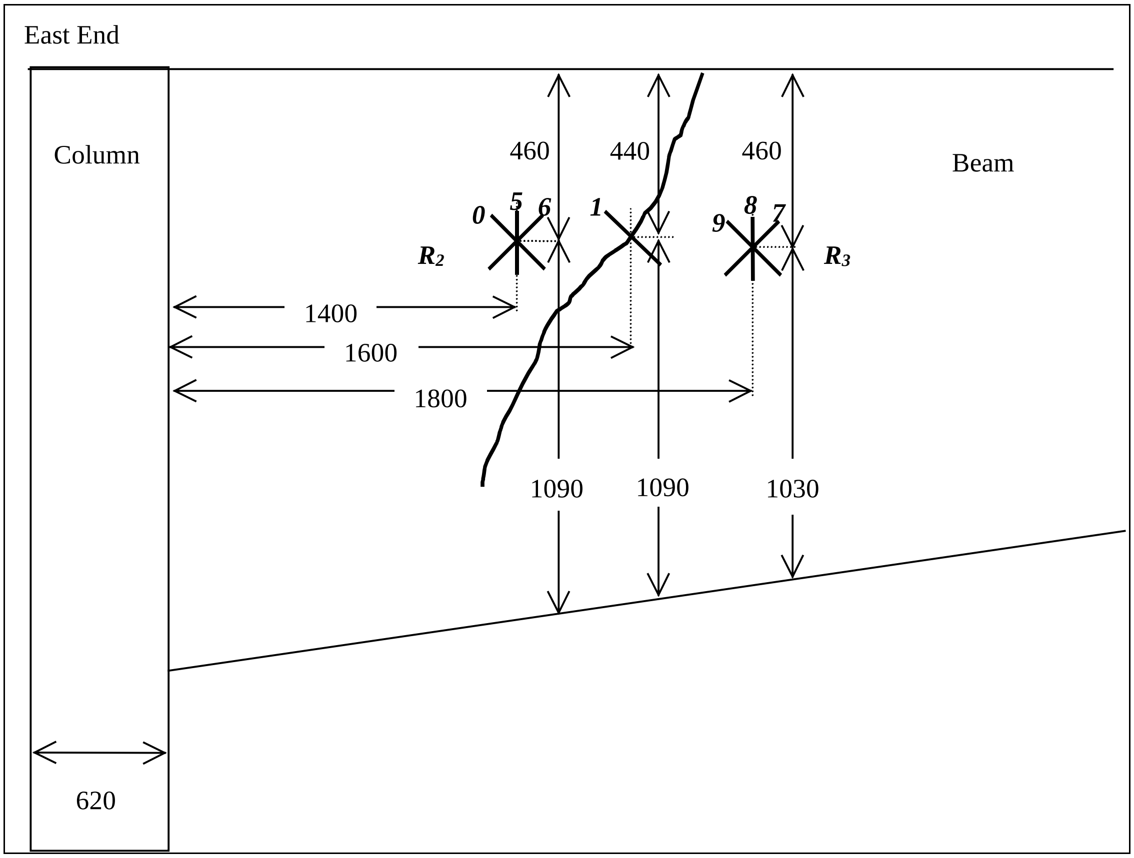

Position of 1000 mm sensors. All dimensions are in millimeters. The italicized numbers are sensor identification numbers.

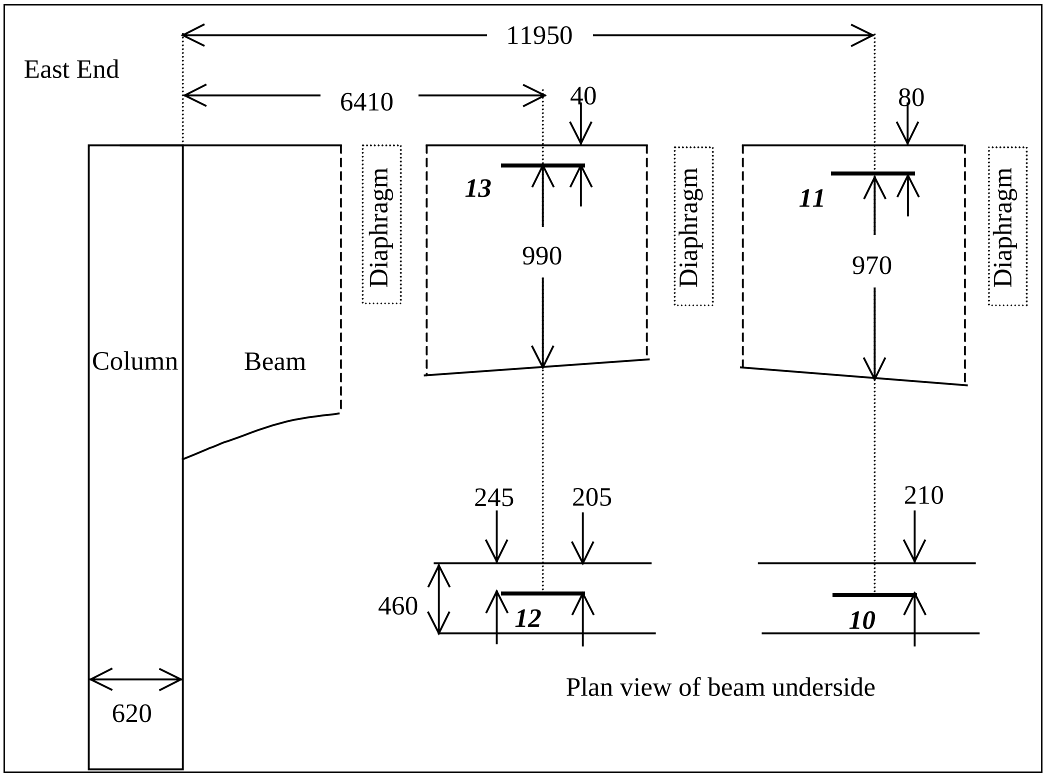

Position of 100 mm sensors on beam 5. All dimensions are in millimeters. The italicized numbers are sensor identification numbers, and the italicized R is the rosette identification label.

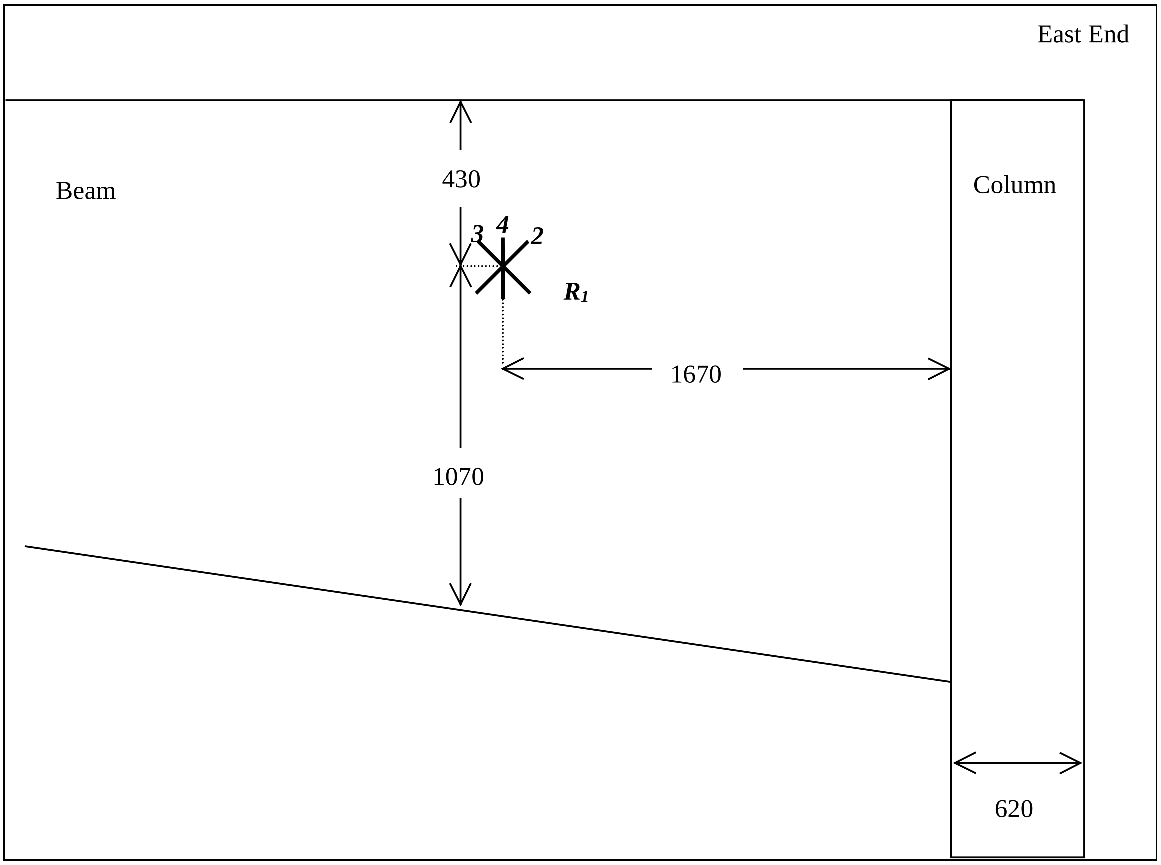

Appendix D3: Data manipulation method

The data manipulation routine used for the Sylvan Bridge data is illustrated below for sensor 3, run 1. Generally, the raw strain data exhibited time-dependent drift. Fast Fourier Transform smoothing with 2000 points was used to construct a curve that represented the baseline for the data. The FFT curve was subtracted from the raw strain data to yield transformed data centered at zero. Savitzky-Golay smoothing with 51 points and a polynomial order of two was used to reduce the noise and define the strain signal due to traffic. The first 50 seconds were truncated in the completed plots to eliminate an artifact of the FFT smoothing process. The data manipulation was conducted with Origin 6.0.

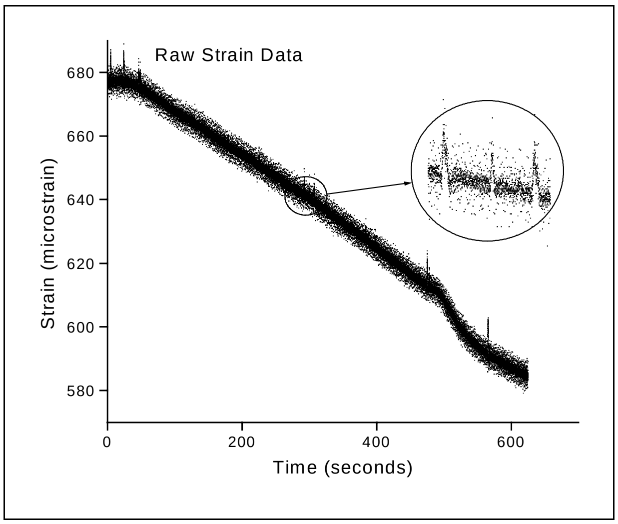

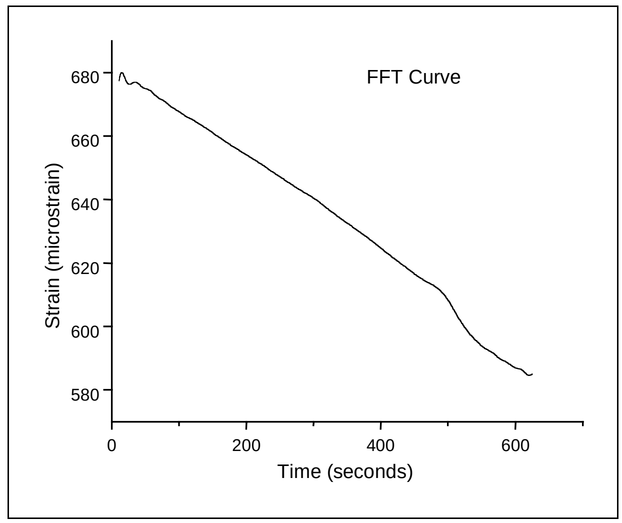

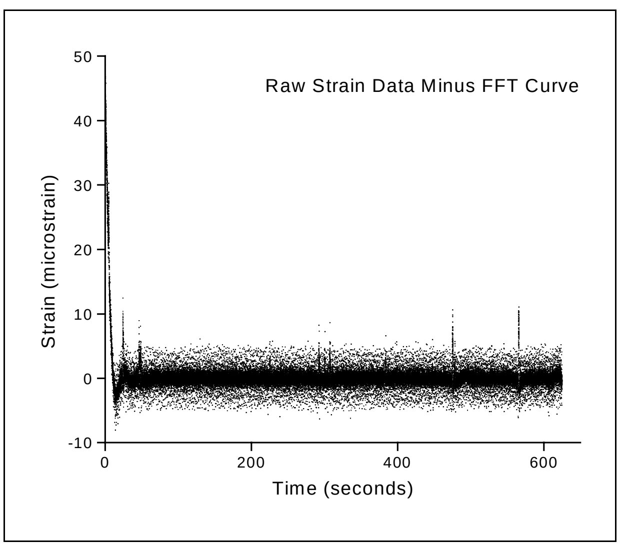

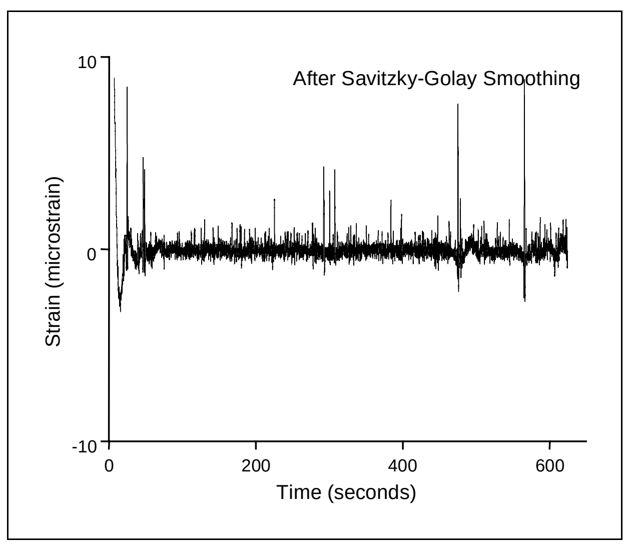

Appendix D4: Strain results

Sets of four sensors were monitored for periods of ten minutes. The sensor numbers (refer to Appendix D) in each set were as follows: (1, 2, 3, 4); (1, 2, 5, 6); (1, 7, 8, 9); (10, 11, 12, 13). Sensor 0 was not operational. The data from the sensors after the data manipulation described in Appendix E are shown below.

Run 1

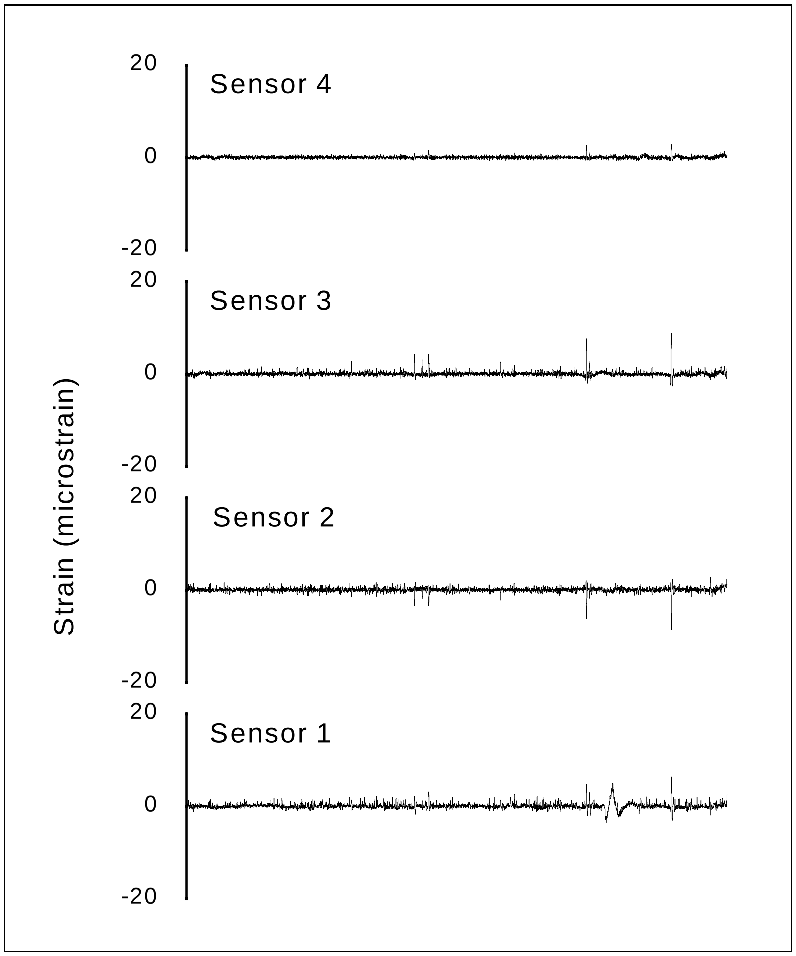

Run 2

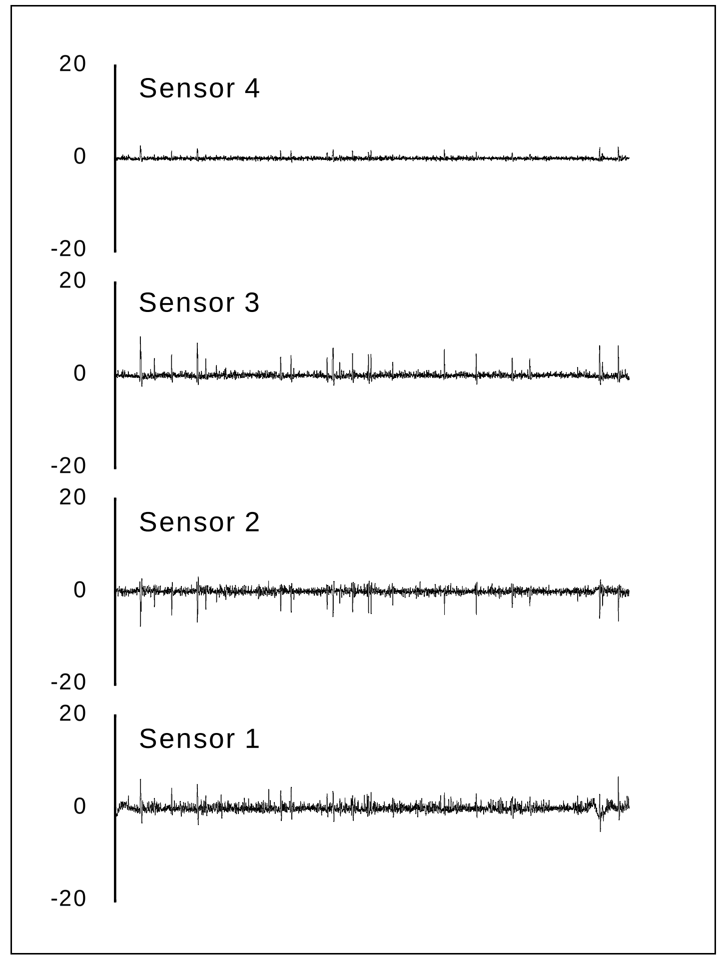

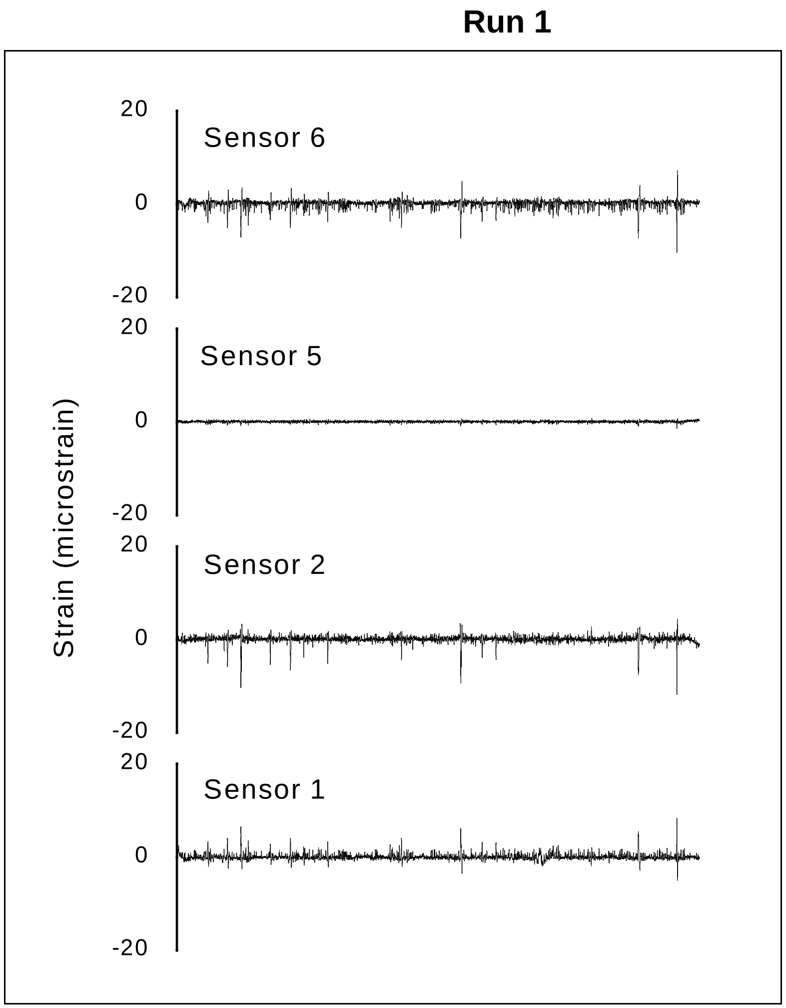
Run 1
Strain (microstrain)
20
Sensor 6
0
-20
20
Sensor 5
0
-20
20
Sensor 2
0
-20
20
Sensor 1
0
-20

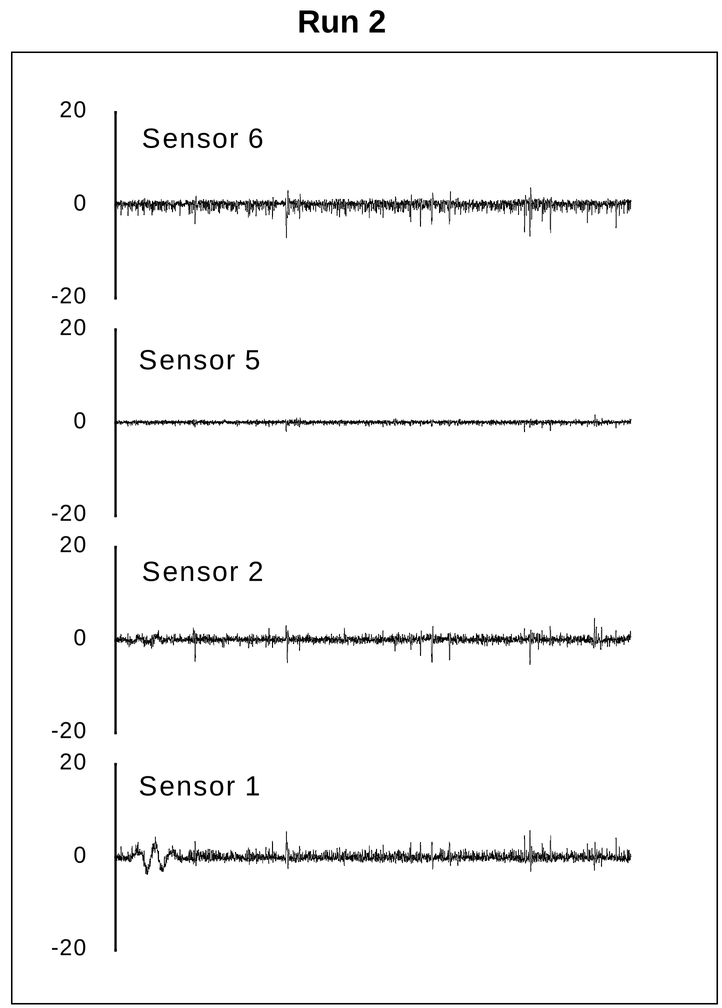
Run 2
20
Sensor 6
0
-20
20
Sensor 5
0
-20
20
Sensor 2
0
-20
20
Sensor 1
0
-20

Run 1

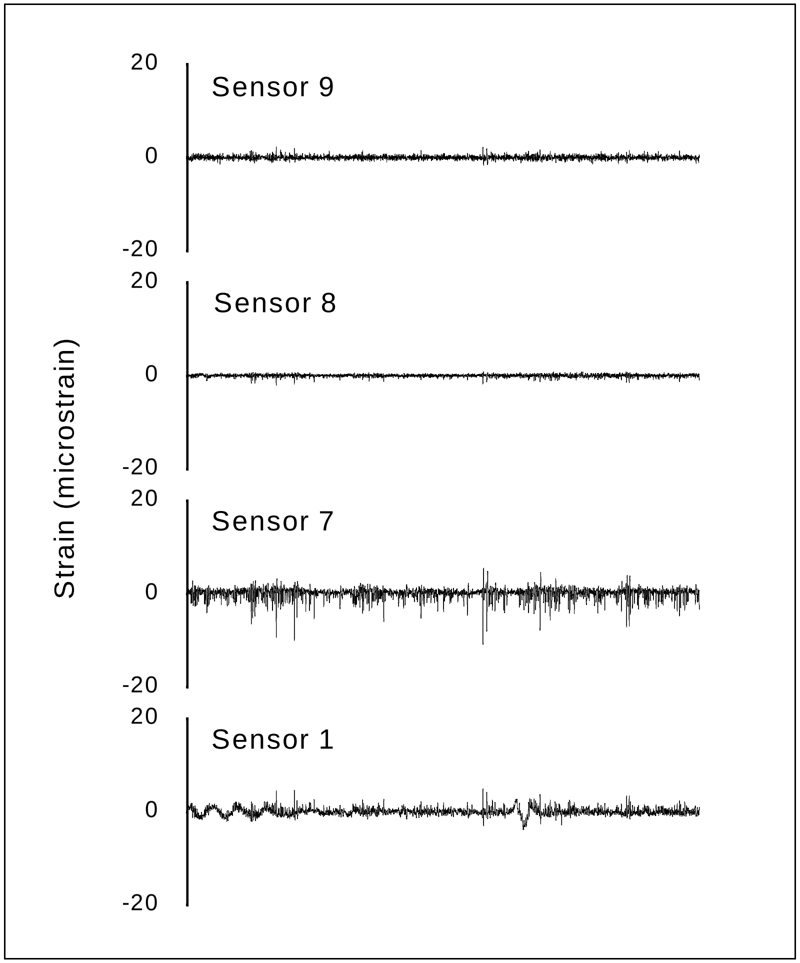

Strain (microstrain)
20
0
-20
Sensor 9
Sensor 8
Sensor 7
Sensor 1

Run 2

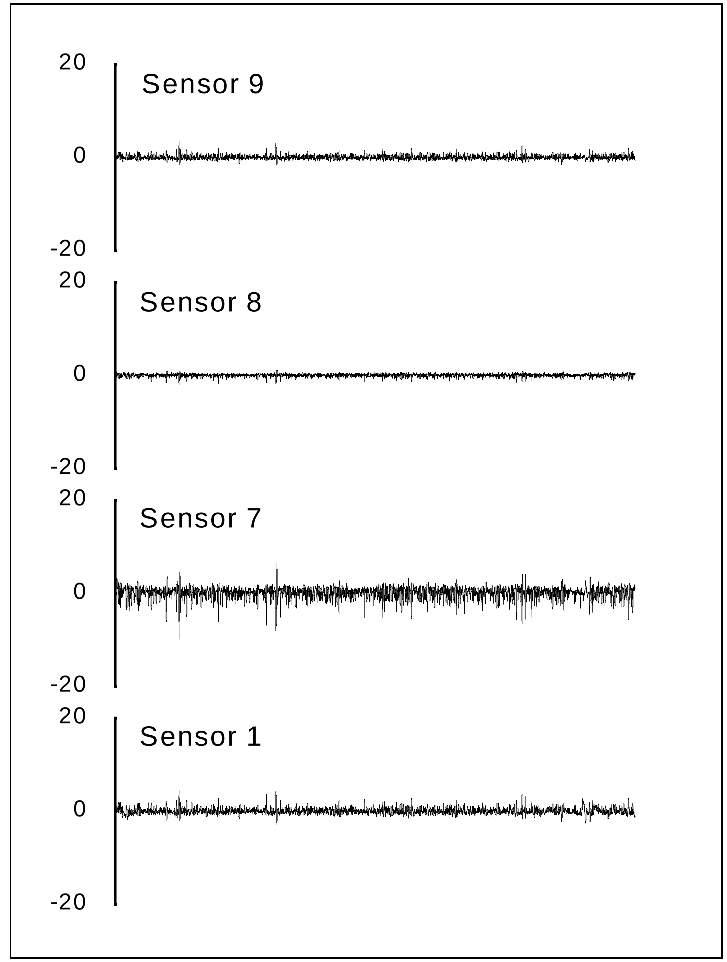

20
0
-20
Sensor 9
Sensor 8
Sensor 7
Sensor 1

Run 1

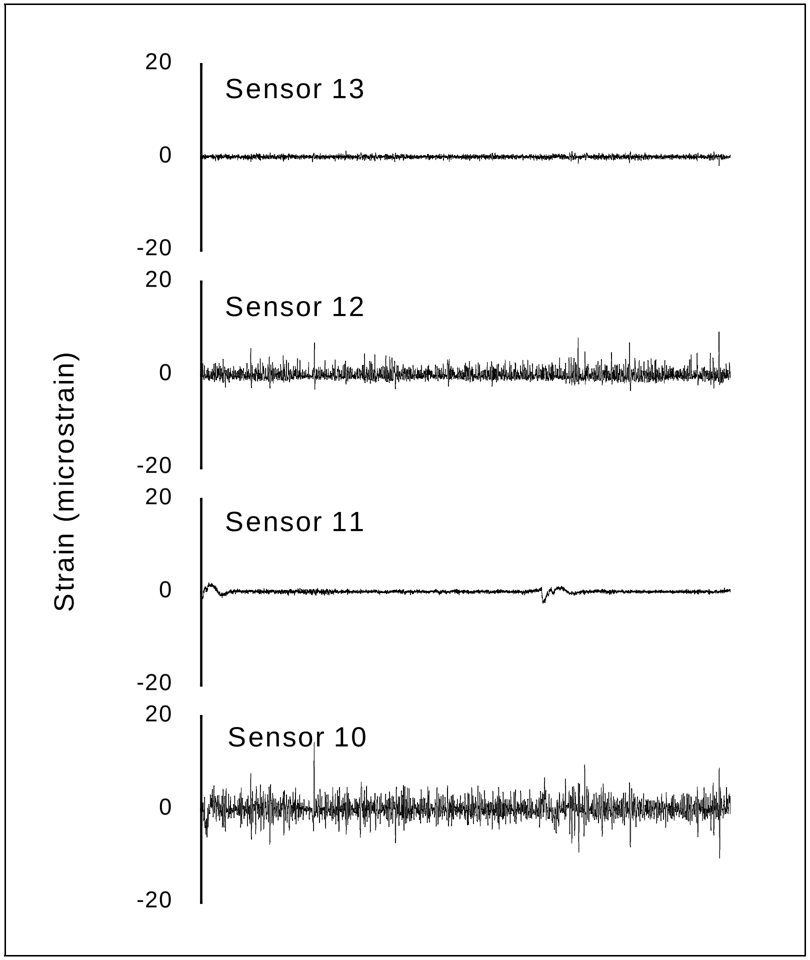
Strain (microstrain)
20
0
-20
Sensor 13
Sensor 12
Sensor 11
Sensor 10

Run 2

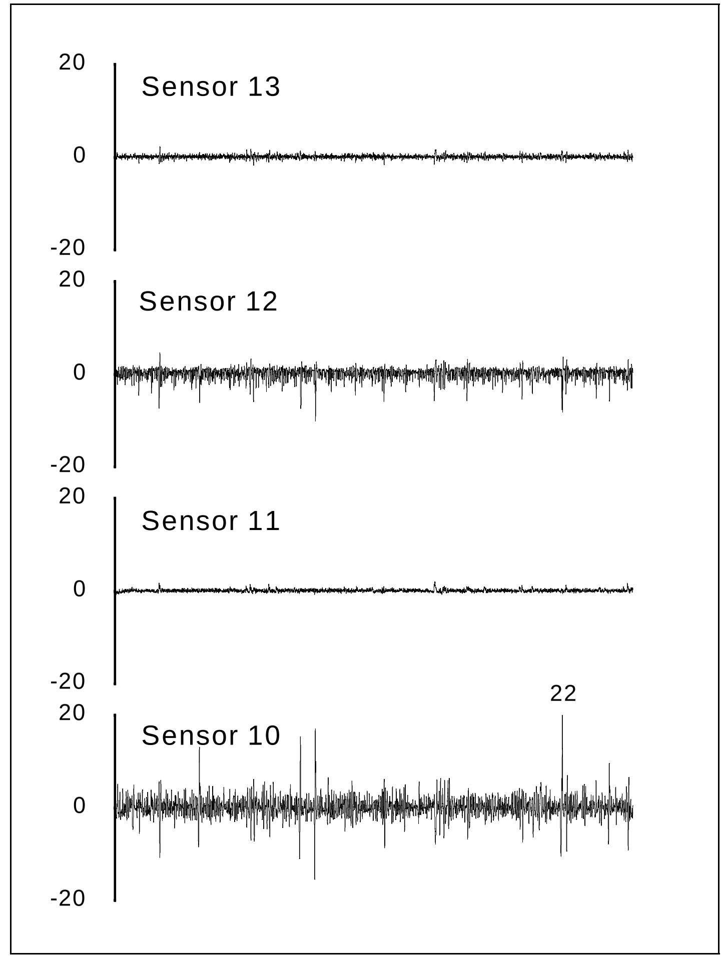
20
0
-20
Sensor 13
Sensor 12
Sensor 11
Sensor 10
22